Metallosupramolecular Cluster Assemblies based on Donor–Acceptor Type Structural Frameworks. Syntheses, Crystal Structures and Spectroscopic Properties of Novel Triosmium Alkylidyne Carbonyl Clusters bearing Remote Ferrocenyl Units as Electron Donors†

Wai-Yeung Wong, Wing-Tak Wong* and Kung-Kai Cheung
Department of Chemistry, The University of Hong Kong, Pokfulam Road, Hong Kong

Two pyridyl ligands containing redox-active ferrocenyl groups $[Fe(\eta^5\text{-}C_5H_5)(\eta^5\text{-}C_5H_4C_6H_4R)]$ [R = C_5H_4N **I** or $NCH(C_5H_4N)$ **II**] have been prepared using a palladium-catalysed aromatic cross-coupling reaction. Treatment of the cluster $[Os_3(\mu\text{-}H)_3(CO)_9(\mu_3\text{-}CCl)]$ with one equivalent of 1,8-diazabicyclo[5.4.0]undec-7-ene in the presence of a ten-fold excess of the ferrocenyl ligands **I** and **II** produces the compounds $[Os_3(\mu\text{-}H)_2(CO)_9(\mu_3\text{-}CNC_5H_4R')]$ [R′ = $C_6H_4(\eta^5\text{-}C_5H_4)Fe(\eta^5\text{-}C_5H_5)$ **1**, R′ = $CHNC_6H_4(\eta^5\text{-}C_5H_4)Fe(\eta^5\text{-}C_5H_5)$ **2**] respectively in good yields. Both compounds **1** and **2** exhibit donor-π-acceptor structural frameworks and show considerable negative solvatochromism in their UV/VIS spectra. Unlike **1** and **2** which possess extended donor-π-acceptor nature, the ferrocenylphosphine cluster derivative $[Os_3(\mu\text{-}H)_2(CO)_9\{\mu_3\text{-}CPPh_2(\eta^5\text{-}C_5H_4)Fe(\eta^5\text{-}C_5H_4PPh_2)\}]$ **3** has also been synthesised in moderate yield by the same synthetic route using 1,1′-bis(diphenylphosphino)ferrocene as the nucleophile. The new clusters **1**–**3** have all been fully characterised by both spectroscopic and crystallographic methods. Conceptually, the classification of **1**–**3** as supermolecules is straightforward, since molecular subunits with well defined intrinsic properties can be easily identified, thus affording a new type of covalently linked donor–acceptor system. Both structural features and spectroscopic data for compounds **1**–**3** are fully consistent with a zwitterionic formulation for these supramolecular species. These results suggest that a strong interaction exists between the ferrocenyl moiety and the Os_3C core in their ground states.

Supramolecular systems that contain electronically coupled photo- and/or redox-active sites are of considerable current interest.[1,2] Special emphasis has been placed on multinuclear assemblies capable of intermetallic energy- or electron-transfer processes.[3,4] In this respect, ferrocene-containing molecules are currently attracting a great deal of attention following the report by Green *et al.*[5] of efficient SHG (second harmonic generation) from an acceptor-substituted aryl ferrocene compound. The development of this kind of ferrocenyl chemistry has found applications in areas such as (*a*) molecular sensors to sense the presence of another metal in close proximity to the ferrocenyl group within the molecule,[6–8] (*b*) molecular ferromagnets,[9,10] (*c*) electrochemical agents,[11] (*d*) non-linear optical materials where the ferrocenyl moiety acts as the donor of a donor-π-acceptor system (D-π-A),[12] (*e*) molecular switches in controlling supramolecular assembly[13] and (*f*) liquid-crystalline materials.[14,15]

Recent reports on the importance of ferrocenyl derivatives in heterobimetallic mixed-valence species[16,17] have encouraged us to design a new system possessing 'donor–acceptor' heterometallic characteristics. Previous work by us has shown that the species $[Os_3(\mu\text{-}H)_2(CO)_9(\mu_3\text{-}C)]$ behaves as a good electron sink and is readily trapped by strong nucleophiles.[18,19] So, our present strategy is to make use of pyridine complexes containing the ferrocenyl group as a redox spectator,[20] which may afford new molecules with highly polarisable donor–acceptor properties. For communications between two metal systems, an aromatic pathway is useful and hence the introduction of a suitable aromatic bridge may increase the architectural flexibility. Such systems are especially promising for the design of new supramolecular species, where novel effects should arise on going from the molecular to the supramolecular level.[21] Incorporation into supramolecular arrangements may influence the properties of the individual molecules by orientation and/or perturbation of their electronic properties.

Herein, we report the synthesis and characterisation of a new family of supermolecules derived from the electron-accepting organometallic fragment $[Os_3(\mu\text{-}H)_2(CO)_9(\mu_3\text{-}C)]$ possessing the chromophores *p*-NC_5H_4R' [R′ = $C_6H_4(\eta^5\text{-}C_5H_4)Fe(\eta^5\text{-}C_5H_5)$ or $CHNC_6H_4(\eta^5\text{-}C_5H_4)Fe(\eta^5\text{-}C_5H_5)$] or $[Fe(\eta^5\text{-}C_5H_4PPh_2)_2]$ as the co-ordinated ligands. The molecular structures of these compounds have been established by single-crystal X-ray analysis.

Results and Discussion

Synthesis.—4-(*p*-Ferrocenylphenyl)pyridine **I** and *p*-ferrocenyl-*N*-(4-pyridylmethylene)aniline **II** (Fig. 1) were prepared respectively by anchoring a ferrocenyl moiety on 4-(*p*-bromophenyl)pyridine and *p*-bromo-*N*-(4-pyridylmethylene)aniline. The one-step palladium-catalysed aromatic cross-coupling reaction with organozinc reagent was employed,[22] *i.e.* ferrocenylzinc chloride was treated with 1 equivalent of the appropriate *para*-substituted bromo derivative in the presence of a palladium(0) catalyst prepared *in situ* (Scheme 1). The ferrocenyl ligands **I** and **II** were isolated as orange solids and have been characterised by elemental analyses, ^1H NMR spectroscopy and FAB mass spectroscopy.

$$ZnCl(\eta^5\text{-}C_5H_4)Fe(\eta^5\text{-}C_5H_5) + RBr \xrightarrow{Pd^0} R(\eta^5\text{-}C_5H_4)Fe(\eta^5\text{-}C_5H_5) + ZnClBr$$

Scheme 1 R = 4-(*p*-C_6H_4)C_5H_4N **I** or 4-(*p*-$C_6H_4N{=}CH$)C_5H_4N **II**

---

† *Supplementary data available:* see Instructions for Authors, *J. Chem. Soc., Dalton Trans.*, 1995, Issue 1, pp. xxv–xxx.

The reaction of the cluster $[Os_3(\mu\text{-}H)_3(CO)_9(\mu_3\text{-}CCl)]$ with 1 equivalent of 1,8-diazabicyclo[5.4.0]undec-7-ene (dbu) in the presence of a 10-fold excess of the required ferrocenyl nucleophiles **I**, **II** and $[Fe(\eta^5\text{-}C_5H_4PPh_2)_2]$ (dppf) gives $[Os_3(\mu\text{-}H)_2(CO)_9(\mu_3\text{-}CNC_5H_4R')]$ [$R' = C_6H_4(\eta^5\text{-}C_5H_4)Fe(\eta^5\text{-}C_5H_5)$ **1** or $CHNC_6H_4(\eta^5\text{-}C_5H_4)Fe(\eta^5\text{-}C_5H_5)$ **2**] and $[Os_3(\mu\text{-}H)_2(CO)_9\{\mu_3\text{-}CPPh_2(\eta^5\text{-}C_5H_4)Fe(\eta^5\text{-}C_5H_4PPh_2)\}]$ **3** respectively in moderate to good yields.[18,19]

Supramolecular Properties.—The systems under consideration they can be viewed as supermolecules, since they are composed of molecular subunits that are capable of independent existence. The covalently linked donor–acceptor systems dealt with here are supermolecules of the type A–L–B, in which two active molecular components (A and B) capable of acting (in their ground or excited states) as an electron donor or acceptor are covalently linked *via* a suitable connector (L).[23] Among these, the ferrocenyl (as the electron donor) and triosmium alkylidyne cluster (as the electron acceptor) moieties are certainly the most important components of these supermolecules. For compounds **1** and **2**, the known alkylidyne cluster $[Os_3(\mu\text{-}H)_2(CO)_9(\mu_3\text{-}CNC_5H_5)]$[19,24] and the ferrocene act as the electron-acceptor and -donor respectively. For **3**, the cluster $[Os_3(\mu\text{-}H)_3(CO)_9(\mu_3\text{-}CH)]$[25] and the diphenylphosphinoferrocene[26] play the corresponding roles. These electron donors and acceptors are bridged by suitable spacers (L = C_6H_6 **1**, $C_6H_5NCH_2$ **2**, $HPPh_2$ **3**), thus providing covalently linked donor-acceptor systems with well defined donor–acceptor distance and geometry.

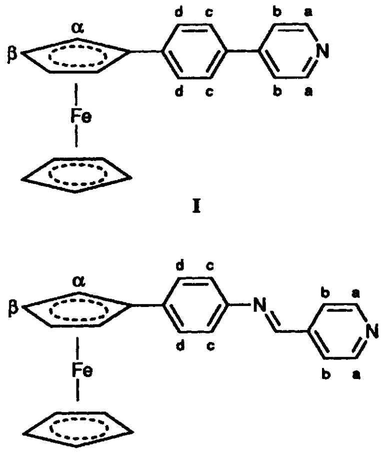

I

II

Fig. 1 Structural formulae of **I** and **II**

With respect to the electronic configurations, such covalently linked donor–acceptor systems undergo spontaneous intercomponent electron-transfer processes, affording fully charge-separated species $A^+\text{–}L\text{–}B^-$ (Fig. 2). In fact, two of these molecules **1** and **2** contain the highly polarisable donor-π-acceptor (D-π-A) structural motif and their corresponding charge-separated canonical forms **a** and **b** are shown.

Spectroscopic Characterisation.—The spectroscopic data (IR, ^1H NMR and MS) for the three new compounds are fully consistent with the solid-state structures. These compounds have many common spectral features. The solution IR spectra in the region 2200–1600 cm^{-1} show similar spectral patterns to the reported system[18,19] and hence they are isostructural. Moreover, the positive FAB mass spectra of **1**–**3** show the

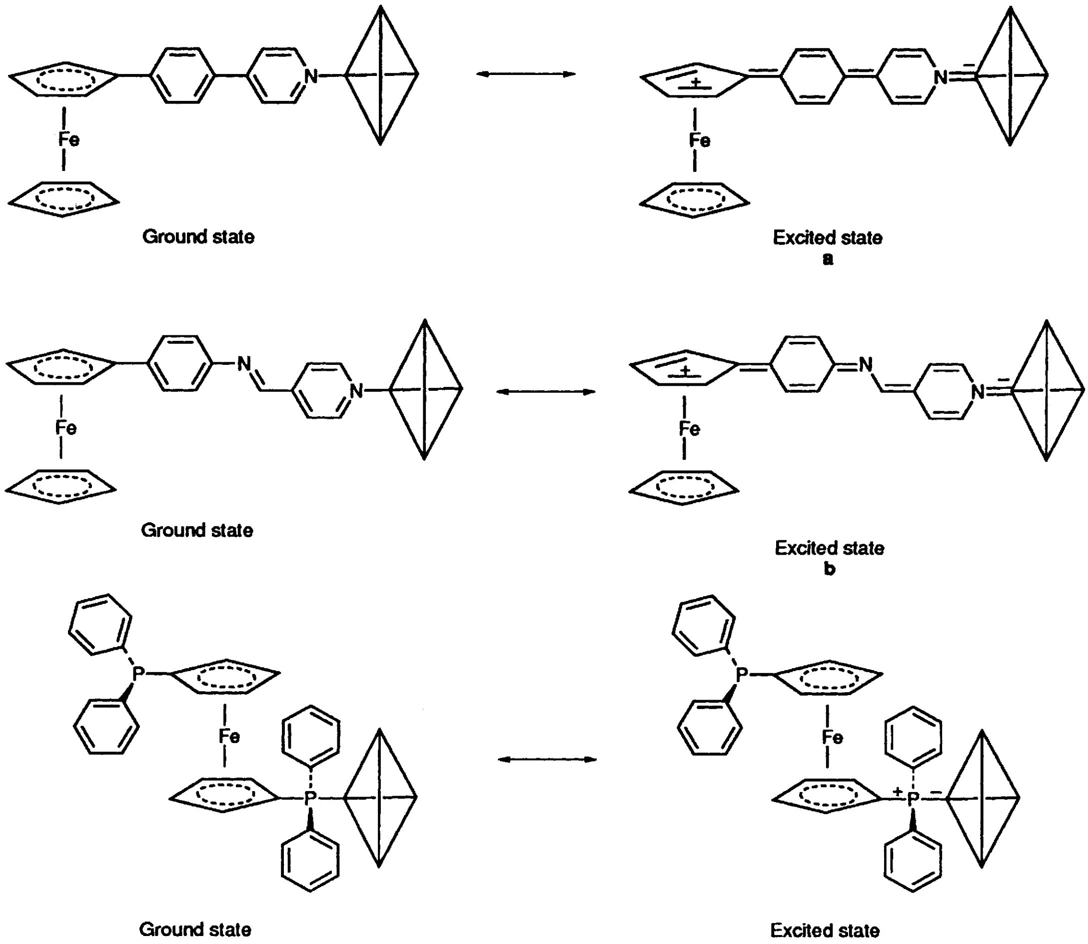

Fig. 2 Zwitterionic formulations for compounds **1**–**3**

parent ions at m/z = 1177, 1204 and 1392 respectively. Furthermore, each of these shows the stepwise losses of nine carbonyls.

The ^1H NMR spectral patterns due to the organic moieties for **1**–**3** are very similar to those of the corresponding free ligands. However, the chemical shifts are found to be downfield for the clusters. In particular, the introduction of the cluster unit can cause downfield shifts as large as *ca.* 1.0 ppm (proton H_a in **1** and **2**). These results are in good agreement for ferrocenyl moieties co-ordinated to electron-withdrawing cluster frameworks. Compounds **1** and **2** show a singlet and **3** a doublet with J(P–H) = 2.8 Hz in the hydride region of the ^1H NMR spectrum in the range δ −18 to −20. Typical AA'BB' spectral patterns with two pairs of doublets of equal intensities appear in the ^1H NMR spectra of both **1** and **2**. The ferrocenyl ligands in compounds **1** and **2** give rise to the expected patterns where the unsubstituted C_5H_5 ring gives a strong singlet at essentially the same position as the ligands **I** and **II** themselves and the monosubstituted C_5H_4 ring gives an unsymmetrical pair of triplets corresponding to the spectrum of an A_2B_2 case with J(adjacent) ≅ J(cross). These triplets appear at the low-field side of the C_5H_5 singlet, showing that all four ring protons are deshielded by the aryl ring bearing the ferrocenyl donors. The exact positions of these triplets change to a very small extent (up to *ca.* 0.06 ppm) with variation of the aryl substituents. However, ^1H–^{31}P coupling causes a rather complicated pattern for the C_5H_4 rings in **3**. The ^{31}P-{^1H} NMR spectrum of **3** in CD_2Cl_2 shows two singlet signals at δ −17.04 and 41.82. This suggests that the two phosphorus atoms are in completely different environments and an unsymmetrical arrangement of the diphenylphosphino moieties in **3** is expected. The corresponding signal of the free ligand itself, [Fe(η^5-$C_5H_4PPh_2)_2$], under the same conditions appears at δ −15.22. The downfield ^{31}P signal is assigned to the phosphorus atom directly attached to the apical carbon of the cluster unit where partial positive charge has been created by the electron-withdrawing Os_3C core.

Molecular Structures of Compounds **1**·$CHCl_3$, **2** *and* **3**.—The molecular structure of compound **1** together with the atomic labelling scheme is depicted in Fig. 3, while selected bond lengths and angles are summarised in Table 1. In the solid state, compound **1** consists of a triosmium alkylidyne metal core arrangement with a 4-(*p*-ferrocenylphenyl)pyridine moiety bonded to the μ_3-bridging alkylidyne carbon atom. Structurally, **1** can be treated as having an alkylidyne cluster [$Os_3(\mu$-H$)_2(CO)_9(\mu_3$-CNC$_5H_5)$] which is linked to the ferrocene by the phenyl ring. The two metal hydrides that show up in the ^1H NMR spectrum of **1** cannot be located directly by X-ray analysis. However, potential-energy calculations suggested that one bridges the Os(1)–Os(2) edge and the other the Os(1)–Os(3) edge.[27] These two edges (average length 2.879 Å) are significantly longer than the Os(2)–Os(3) bond [2.778(1) Å]. The Os–C(alkylidyne) bond lengths are essentially equivalent (average 2.10 Å). Slight shortenings of C(13)–C(16) and C(19)–C(22) bonds are observed [1.46(2) and 1.45(2) Å respectively] which is consistent with the partial conjugation effect (Fig. 2). The dihedral angle between the η^5-C_5H_4 and η^5-C_5H_5 planes in the ferrocenyl ligand is 2.4°. The C_5H_4 and C_5H_5 fragments of the ferrocenyl group deviate from the staggered conformation by 5.5°. The phenyl ring is rotated by 25.5° relative to the plane of the attached pyridine ring about the C–C linking bond. The dihedral angle between the phenyl plane and the C_5H_4 ring is 4.5°.

The molecular structure of compound **2** together with the atomic labelling scheme is shown in Fig. 4. Some important bond lengths and angles are given in Table 2. The basic metal cluster core unit is essentially identical to that observed in **1**. The non-bridged Os–Os bond length for **2** [Os(2)–Os(3) 2.7719(8) Å] is shorter than 2.887(3) Å observed in the parent binary carbonyl [$Os_3(CO)_{12}$],[28] while the mean distance (2.871 Å) for the hydride-bridged Os–Os bonds is comparable to that observed in [$Os_3(CO)_{12}$]. The metal–alkylidyne carbon bond lengths (average 2.10 Å) are typical of those in **1** and the alkylidyne clusters already structurally characterised.[18,19] The C=N bond length is 1.13(2) Å. The two cyclopentadienyl rings are almost parallel and the dihedral angle between the C_5H_4 and C_5H_5 planes is only 0.6°. The ferrocenyl group in **2** is nearly staggered and the deviation of the five-membered rings from the

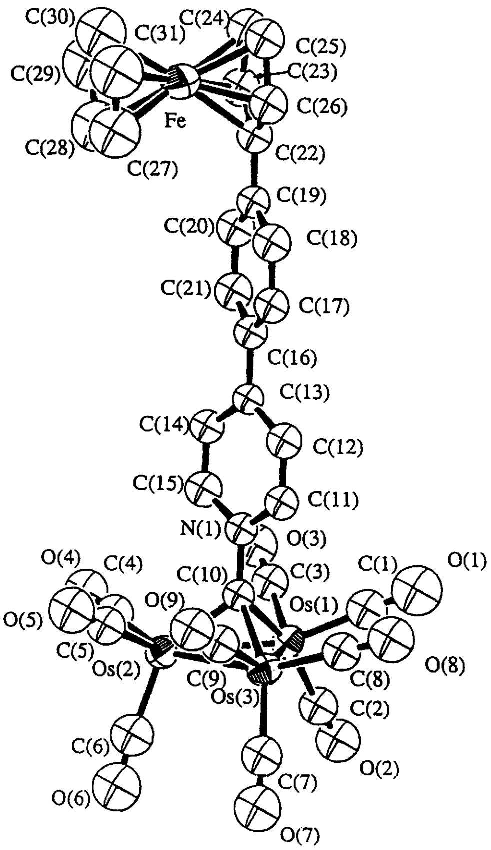

Fig. 3 The molecular structure of [$Os_3(\mu$-H$)_2(CO)_9\{\mu_3$-CNC$_5H_4C_6H_4(\eta^5$-$C_5H_4)$Fe$(\eta^5$-$C_5H_5)\}$] **1**

Table 1 Selected bond lengths (Å) and angles (°) for compound **1**

Os(1)–Os(2)	2.8785(9)	Os(1)–Os(3)	2.8803(8)
Os(2)–Os(3)	2.778(1)	Os(1)–C(10)	2.12(1)
Os(2)–C(10)	2.08(1)	Os(3)–C(10)	2.09(1)
N(1)–C(10)	1.44(1)	C(13)–C(16)	1.46(2)
C(19)–C(22)	1.45(2)	Fe–C(22)	2.04(1)
Fe–C(23)	2.02(1)	Fe–C(24)	2.03(2)
Fe–C(25)	2.04(2)	Fe–C(26)	2.01(1)
Fe–C(27)	2.03(2)	Fe–C(28)	2.04(2)
Fe–C(29)	2.03(2)	Fe–C(30)	2.03(2)
Fe–C(31)	2.05(2)	Fe–ring(C_5H_5)	1.673
Fe–ring(C_5H_4)	1.642		
Os(2)–Os(1)–Os(3)	57.69(2)	Os(1)–Os(2)–Os(3)	61.19(2)
Os(1)–Os(3)–Os(2)	61.12(2)	Os(1)–C(10)–Os(2)	86.6(5)
Os(1)–C(10)–Os(3)	86.4(4)	Os(2)–C(10)–Os(3)	83.5(5)
C(10)–N(1)–C(11)	122(1)	C(10)–N(1)–C(15)	120(1)
C(13)–C(16)–C(17)	122(1)	C(13)–C(16)–C(21)	121(7)
C(19)–C(22)–C(23)	127(1)	C(19)–C(22)–C(26)	127(1)

Angles between planes

A and B	25.5	A and C	30.0
B and C	4.5	C and D	2.4

Planes: A, defined by atoms N(1)–C(11)–C(12)–C(13)–C(14)–C(15); B, C(16)–C(17)–C(18)–C(19)–C(20)–C(21); C, C(22)–C(23)–C(24)–C(25)–C(26); D, C(27)–C(28)–C(29)–C(30)–C(31).

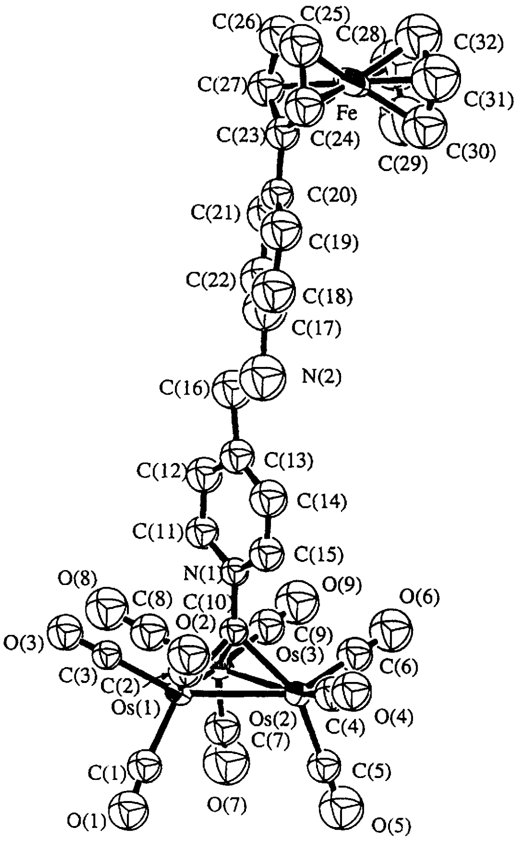

Fig. 4 The molecular structure of [$Os_3(\mu\text{-}H)_2(CO)_9\{\mu_3\text{-}CNC_5H_4CH{=}NC_6H_4(\eta^5\text{-}C_5H_4)Fe(\eta^5\text{-}C_5H_5)\}$] **2**

Table 2 Selected bond lengths (Å) and angles (°) for compound **2**

Os(1)–Os(2)	2.8679(8)	Os(1)–Os(3)	2.8733(6)
Os(2)–Os(3)	2.7719(8)	Os(1)–C(10)	2.12(1)
Os(2)–C(10)	2.09(1)	Os(3)–C(10)	2.09(1)
N(1)–C(10)	1.47(2)	C(13)–C(16)	1.60(3)
N(2)–C(16)	1.13(2)	N(2)–C(17)	1.63(4)
C(20)–C(23)	1.48(2)	Fe–C(23)	2.07(2)
Fe–C(24)	2.05(2)	Fe–C(25)	2.05(3)
Fe–C(26)	2.03(3)	Fe–C(27)	2.06(2)
Fe–C(28)	2.04(2)	Fe–C(29)	2.07(3)
Fe–C(30)	2.01(2)	Fe–C(31)	2.03(2)
Fe–C(32)	1.99(2)	Fe–ring(C_5H_5)	1.646
Fe–ring(C_5H_4)	1.663		
Os(2)–Os(1)–Os(3)	57.74(2)	Os(1)–Os(2)–Os(3)	61.23(2)
Os(1)–Os(3)–Os(2)	61.03(2)	Os(1)–C(10)–Os(2)	85.9(5)
Os(1)–C(10)–Os(3)	86.2(5)	Os(2)–C(10)–Os(3)	83.1(6)
C(10)–N(1)–C(11)	121(2)	C(10)–N(1)–C(15)	121(1)
N(2)–C(16)–C(13)	107(2)	C(16)–N(2)–C(17)	109(2)
C(20)–C(23)–C(24)	127(1)	C(20)–C(23)–C(27)	126(1)

Angles between planes

A and B	33.6	A and C	17.9
B and C	15.9	C and D	0.6

Planes: A, defined by atoms N(1)–C(11)–C(12)–C(13)–C(14)–C(15); B, C(17)–C(18)–C(19)–C(20)–C(21)–C(22); C, C(23)–C(24)–C(25)–C(26)–C(27); D, C(28)–C(29)–C(30)–C(31)–C(32).

staggered conformation is 3.2°. The dihedral angle between the pyridine and phenyl rings is 33.6° whilst the corresponding angle between the phenyl and C_5H_4 rings is 15.9°. The C=N bond is out of the best plane formed by the pyridine atoms with the distance of N(2) from the plane being 0.17 Å. The N(2) atom is found to be on the same side of the pyridine as well as the phenyl rings. However, C(16) lies between them.

Table 3 Selected bond lengths (Å) and angles (°) for compound **3**

Os(1)–Os(2)	2.8839(9)	Os(1)–Os(3)	2.7476(9)
Os(2)–Os(3)	2.8885(9)	Os(1)–C(10)	2.12(1)
Os(2)–C(10)	2.13(1)	Os(3)–C(10)	2.16(1)
P(1)–C(10)	1.72(1)	P(1)–C(11)	1.82(2)
P(1)–C(17)	1.80(1)	P(1)–C(23)	1.79(1)
Fe–C(23)	2.06(1)	Fe–C(24)	2.02(2)
Fe–C(25)	2.05(2)	Fe–C(26)	2.05(2)
Fe–C(27)	2.07(1)	Fe–C(28)	2.04(2)
Fe–C(29)	2.04(2)	Fe–C(30)	2.04(2)
Fe–C(31)	2.05(2)	Fe–C(32)	2.06(2)
P(2)–C(31)	1.83(2)	P(2)–C(33)	1.82(2)
P(2)–C(39)	1.82(2)	Fe–ring(C_5H_4)	1.662
Fe–ring(C_5H_4)	1.658		
Os(2)–Os(1)–Os(3)	61.66(2)	Os(1)–Os(2)–Os(3)	56.85(2)
Os(1)–Os(3)–Os(2)	61.49(2)	Os(1)–C(10)–Os(2)	85.5(5)
Os(1)–C(10)–Os(3)	79.8(5)	Os(2)–C(10)–Os(3)	84.7(5)
C(10)–P(1)–C(23)	112.3(7)	C(11)–P(1)–C(23)	103.5(7)
C(17)–P(1)–C(23)	111.7(7)	C(31)–P(2)–C(33)	102.0(7)
C(31)–P(2)–C(39)	100.4(7)		

Angle between planes

A and B	5.5

Planes: A, defined by atoms C(23)–C(24)–C(25)–C(26)–C(27); B, C(28)–C(29)–C(30)–C(31)–C(32).

Table 4 Electronic absorption spectral data for the clusters **1**, **2** and **3** and their corresponding free ligands

	λ_{max}/nm (10^{-3} ε/dm^3 mol^{-1} cm^{-1})			
Compounds	C_6H_{14}	$CHCl_3$	CH_2Cl_2	Me_2CO
I			265 (12.7)	
			301 (14.8)	
			357 (2.72)	
			456 (0.86)	
II			326 (2.41)	
			450 (sh) (0.89)	
dppf			441 (0.81)	
1	408 (2.92)	413 (2.96)	421 (3.36)	408 (3.84)
	451 (2.88)	544 (4.23)	533 (4.81)	509 (4.20)
	564 (4.51)			
2	397 (3.76)	404 (2.97)	403 (4.56)	392 (3.99)
	507 (3.09)	612 (3.74)	597 (5.33)	555 (4.22)
	643 (4.83)			
3			444*	

* Band is a shoulder on a more intense band.

A perspective view of the molecular structure of compound **3** together with the atomic labelling scheme is depicted in Fig. 5. Relevant bond parameters are listed in Table 3. Compound **3** contains an alkylidyne metal core having the 1,1′-bis(diphenylphosphino)ferrocene moiety co-ordinated directly through one phosphorus atom to the apical carbon atom. The average Os–C(alkylidyne) bond distance is 2.14 Å. The two edges [Os(1)–Os(2) 2.8839(9) and Os(2)–Os(3) 2.8885(9) Å] are bridged by hydride atoms and the non-bridged Os(1)–Os(3) bond length is 2.7476(9) Å. The average C–C bond length in both cyclopentadienyl rings is 1.415 Å, which is in good agreement with the values reported for other ferrocene derivatives.[29] The two substituted η^5-C_5H_4 fragments of the ferrocenyl unit deviate from the eclipsed conformation by 11.3°. Many examples of deviations of ferrocenyl groups from the staggered conformation are known.[29,30] There is also a small C_5H_4 ring tilt of 5.5°.

Electronic Absorption Spectra.—Table 4 presents data for the electronic absorption spectra in solvents of different polarity in the range 300–750 nm for clusters **1**–**3** together with data for the

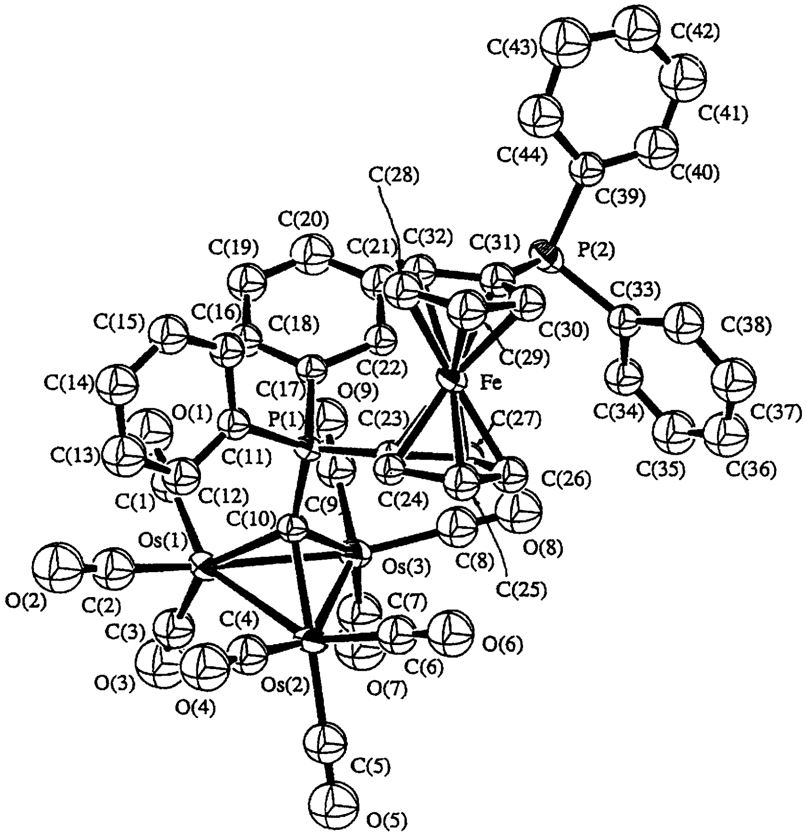

Fig. 5 The molecular structure of $[Os_3(\mu\text{-}H)_2(CO)_9\{\mu_3\text{-}CPPh_2(\eta^5\text{-}C_5H_4)Fe(\eta^5\text{-}C_5H_4PPh_2)\}]$ **3**

corresponding ferrocenyl ligands in CH_2Cl_2. A variety of colours (deep red **1**, deep blue **2**, orange-yellow **3**) are displayed by the three compounds in their solid states. For **1** and **2**, there are essentially two bands in this range. Of the D-π-A type complexes, strong negative solvatochromic shifts are observed for the low-energy bands in both **1** and **2**. Fenske–Hall molecular orbital calculations of these complexes suggested that the highest occupied molecular orbital (HOMO) is largely metal-based whereas the lowest unoccupied molecular orbital (LUMO) is mostly dominated by the organic moiety.[31] These calculations allow us to assign tentatively the low-energy metal-to-ligand charge-transfer (m.l.c.t.) transition which accounts for the intense colours exhibited by both compounds **1** and **2**. The m.l.c.t. absorption blue shifts in progressively more polar solvent media[32] and the effects these solvents have on the energy of the m.l.c.t. transitions suggest a less polar excited state upon photoexcitation. Another important feature shown from the data is that λ_{max} for the low-energy band in **2** is larger than the corresponding value in **1**. Probably, a more extensive conjugation through the C=N bond in **2** reduces the energy gap between the HOMO and LUMO and hence results in a decreased transition energy in **2**. However, the high-energy band does not show any marked solvent effect.

The orange colours of the free ferrocenyl ligands **I** and **II** are due to the presence of the ferrocenyl groups [$\lambda_{max}(CH_2Cl_2)$ 456, ε 860, **I**; $\lambda_{max}(CH_2Cl_2)$ 450 nm, ε 890 $dm^3\ mol^{-1}\ cm^{-1}$, **II**]. Because of its relatively small absorption coefficient, the ferrocenyl absorption in the visible region cannot be easily discerned in the spectra.

Complex **3** which is orange-yellow in solution exhibits a shoulder at 444 nm in CH_2Cl_2. The ligand $[Fe(\eta^5\text{-}C_5H_4PPh_2)_2]$ shows an absorption band at λ_{max} 441 nm (ε 810 $dm^3\ mol^{-1}\ cm^{-1}$) in the same solvent. The origin of the shoulder cannot be discerned since it may arise either from a m.l.c.t. transition or the ferrocenyl absorption.

Conclusion

Two monosubstituted ferrocenyl complexes bearing pendant pyridyl groups **I** and **II** have been prepared together with three novel supramolecular species (**1**, **2** and **3**). Two of these supermolecules (**1** and **2**) possess the donor-π-acceptor structural motif with variable spacers and they exhibit unusually large negative solvatochromism.

Experimental

Materials and Methods.—None of the compounds reported is particularly air-sensitive, but all reactions were performed under an atmosphere of dry dinitrogen. All solvents were dried over appropriate reagents and distilled before use. All chemicals, except where stated, were purchased from commercial sources and used as received. The compounds $[Fe(\eta^5\text{-}C_5H_5)(\eta^5\text{-}C_5H_4Br)]$,[33] 4-(*p*-bromophenyl)pyridine[34] and $[Os_3(\mu\text{-}H)_3(CO)_9(\mu_3\text{-}CCl)]$[35] were prepared by the literature methods. Infrared spectra were recorded on a Bio-Rad FTS-7 IR spectrometer using 0.5 mm solution cells. The NMR spectra were recorded on a JEOL GSX 270FT-NMR spectrometer using deuteriated solvents as lock and reference. Chemical shifts are reported in ppm relative to $SiMe_4$ for ^1H and 85% H_3PO_4 for ^{31}P NMR spectra. Mass spectra were recorded on a Finnigan MAT 95 instrument by the fast-atom bombardment technique. Electronic absorption spectra were obtained in a microprocessor-controlled Perkin-Elmer Lambda 3B UV/VIS spectrophotometer, thermostatted by a Lauda circulating bath. Routine separation of products was performed in air by thin layer chromatography with plates coated with Merck Kieselgel 60 GF_{254}.

Preparation of $[Fe(\eta^5\text{-}C_5H_5)(\eta^5\text{-}C_5H_4C_6H_4C_5H_4N)]$ **I**.—A solution of $[Fe(\eta^5\text{-}C_5H_5)(\eta^5\text{-}C_5H_4Li)]$ was prepared by addition of *n*-butyllithium (2.5 mol dm^{-3} in hexanes, 1.80 cm^3, 4.60 mmol) to bromoferrocene (1.00 g, 3.80 mmol) in diethyl

Table 5 Crystal data and data collection parameters for **1**, **2** and **3**

Compound	**1**·$CHCl_3$	**2**	**3**
Formula	$C_{32}H_{20}Cl_3FeNO_9Os_3$	$C_{32}H_{20}FeN_2O_9Os_3$	$C_{44}H_{30}FeO_9Os_3P_2$
M	1294.9	1202.4	1390.4
Colour, habit	Red, plates	Blue, blocks	Yellow, blocks
Crystal dimensions/mm	0.10 × 0.16 × 0.28	0.14 × 0.18 × 0.32	0.20 × 0.24 × 0.38
Crystal system	Monoclinic	Triclinic	Triclinic
Space group	$P2_1/n$ (no. 14)	$P\bar{1}$ (no. 2)	$P\bar{1}$ (no. 2)
a/Å	8.244(3)	8.199(2)	14.170(2)
b/Å	14.128(8)	14.459(5)	18.286(3)
c/Å	30.931(4)	15.422(2)	9.019(2)
α/°	90.0	112.69(2)	94.57(2)
β/°	91.71(3)	91.89(1)	105.19(1)
γ/°	90.0	98.51(2)	108.82(1)
U/Å^3	3600(2)	1658(1)	2099.9(7)
Z	4	2	2
D_c/g cm^{-3}	2.389	2.408	2.199
μ(Mo-Kα)/cm^{-1}	112.14	119.60	95.11
F(000)	2384	1104	1300
T/K	298	298	296
Scan type	ω–2θ	ω–2θ	ω–2θ
Scan rate in ω/° min^{-1}	16.0	1.03–16.48	16.0
Scan range/°	0.73 + 0.35 tan θ	0.50 + 0.34 tan θ	1.00 + 0.35 tan θ
2θ range/°	2–45	2–45	2–45
Reflections collected	5335	4684	5767
Unique reflections	4931	4316	5497
Observed reflections [$F > n\sigma(F)$]	3395 (n = 6)	3470 (n = 3)	4101 (n = 6)
Absorption correction	ψ-scan	ψ-scan	ψ-scan
Transmission factors	0.5134–1.0000	0.626–0.996	0.6283–1.0000
Weighting scheme $w = [\sigma^2(F^2) + gF^2]^{-1}$	g = 0.002	g = 0.04	g = 0.014
R	0.037	0.041	0.045
R'	0.036	0.057	0.055
Residual electron density (close to Os)/e Å^{-3}	1.52 to −1.13	1.60 to −0.97	1.14 to −2.62

Table 6 Atomic coordinates for compound **1** with estimated standard deviations (e.s.d.s) in parentheses

Atom	x	y	z	Atom	x	y	z
Os(1)	−0.046 10(7)	0.122 08(4)	0.297 08(2)	C(9)	−0.007(2)	−0.192(1)	0.327 5(5)
Os(2)	0.196 49(7)	0.019 56(4)	0.346 88(2)	C(10)	0.079(1)	−0.006 5(9)	0.287 5(4)
Os(3)	−0.095 84(7)	−0.069 40(4)	0.325 79(2)	C(11)	0.059(2)	−0.092 1(10)	0.218 6(5)
Fe	0.747 1(3)	−0.266 9(2)	−0.002 89(8)	C(12)	0.119(2)	−0.117(1)	0.180 0(5)
Cl(1)	0.470 3(9)	0.485 8(6)	0.570 9(3)	C(13)	0.269(1)	−0.083 9(9)	0.165 7(4)
Cl(2)	0.237 1(8)	0.345 7(5)	0.589 2(3)	C(14)	0.352(2)	−0.025 6(10)	0.194 9(5)
Cl(3)	0.499(1)	0.381 8(6)	0.648 0(3)	C(15)	0.292(2)	−0.004(1)	0.234 2(5)
O(1)	−0.291(2)	0.100 8(10)	0.223 3(5)	C(16)	0.335(2)	−0.110 8(10)	0.124 4(5)
O(2)	−0.218(1)	0.293 2(8)	0.337 0(4)	C(17)	0.288(2)	−0.193(1)	0.102 9(5)
O(3)	0.191(1)	0.239 3(8)	0.246 1(4)	C(18)	0.354(2)	−0.220(1)	0.065 1(5)
O(4)	0.494(1)	0.140 2(8)	0.332 4(4)	C(19)	0.468(2)	−0.164(1)	0.045 0(5)
O(5)	0.392(1)	−0.161 9(9)	0.355 5(4)	C(20)	0.510(2)	−0.080(1)	0.065 0(5)
O(6)	0.142(2)	0.034 5(9)	0.443 9(5)	C(21)	0.447(2)	−0.054(1)	0.104 0(5)
O(7)	−0.254(1)	−0.084 7(9)	0.413 4(4)	C(22)	0.535(2)	−0.193(1)	0.004 5(5)
O(8)	−0.378(1)	−0.129 5(9)	0.266 8(4)	C(23)	0.645(2)	−0.144(1)	−0.020 5(5)
O(9)	0.048(1)	−0.267 6(8)	0.329 3(4)	C(24)	0.682(2)	−0.197(1)	−0.056 9(6)
N(1)	0.143(1)	−0.035 4(7)	0.246 8(4)	C(25)	0.600(2)	−0.279(1)	−0.055 6(5)
C(1)	−0.194(2)	0.113(1)	0.251 4(6)	C(26)	0.512(2)	−0.280(1)	−0.016 6(5)
C(2)	−0.157(2)	0.228(1)	0.323 4(5)	C(27)	0.808(3)	−0.339(2)	0.051 4(8)
C(3)	0.097(2)	0.196(1)	0.264 9(5)	C(28)	0.885(3)	−0.261(2)	0.052 2(8)
C(4)	0.380(2)	0.092(1)	0.337 5(5)	C(29)	0.978(3)	−0.249(2)	0.016 2(10)
C(5)	0.317(2)	−0.092(1)	0.351 8(5)	C(30)	0.962(3)	−0.331(2)	−0.005 0(8)
C(6)	0.170(2)	0.033(1)	0.407 2(6)	C(31)	0.851(3)	−0.389(2)	0.015 7(8)
C(7)	−0.198(2)	−0.078(1)	0.379 7(6)	C(32)	0.386(4)	0.404(3)	0.600(1)
C(8)	−0.269(2)	−0.107(1)	0.290 3(5)				

ether (80 cm^3) at −78 °C. The mixture was allowed to warm up to room temperature, and after 1 h, the solvent was evaporated *in vacuo* and the residue redissolved in tetrahydrofuran (thf) (15 cm^3). The resulting red-orange solution was then added to a solution of anhydrous zinc chloride (0.52 g, 3.80 mmol) in thf (5 cm^3). The resulting mixture was stirred for 3 h at room temperature, and added to another mixture containing the palladium catalyst and 4-(*p*-bromophenyl)pyridine, prepared as follows: [$Pd(PPh_3)_2Cl_2$] (0.09 g, 0.13 mmol) suspended in thf (5 cm^3) was treated with a toluene solution of $AlHBu^i_2$ (1.0 mol dm^{-3} in toluene, 0.26 cm^3, 0.26 mmol). To the resulting black solution was then added a solution of 4-(*p*-bromophenyl)pyridine (0.58 g, 2.50 mmol) in thf (10 cm^3). The orange-brown mixture was heated to reflux for 15 min before the addition of the ferrocenyl-zinc chloride solution. It was then refluxed for 20 h. The resulting pink slurry was allowed to cool down to room

Table 7 Atomic coordinates for compound **2** with (e.s.d.s) in parentheses

Atom	x	y	z	Atom	x	y	z
Os(1)	0.304 98(6)	0.110 51(3)	0.379 84(3)	C(10)	0.208(1)	0.247 7(9)	0.424 4(8)
Os(2)	0.071 13(6)	0.191 36(4)	0.511 10(3)	C(11)	0.270(2)	0.369(1)	0.349 1(9)
Os(3)	0.389 09(7)	0.301 99(4)	0.539 25(3)	C(12)	0.220(2)	0.416(1)	0.291(1)
Fe	−0.412 6(3)	0.811 9(2)	0.019 5(2)	C(13)	0.063(2)	0.391(1)	0.246(1)
O(1)	0.414(1)	−0.082 5(9)	0.383 7(8)	C(14)	−0.048(2)	0.313(1)	0.259(1)
O(2)	0.069(1)	0.000 7(9)	0.202 7(8)	C(15)	0.004(2)	0.271(1)	0.318(1)
O(3)	0.583(1)	0.168 3(7)	0.277 6(7)	C(16)	0.042(2)	0.460(1)	0.188(1)
O(4)	−0.250(1)	0.061 7(8)	0.400 3(8)	C(17)	−0.125(3)	0.517(2)	0.109(1)
O(5)	0.080(2)	0.133(1)	0.682 8(9)	C(18)	−0.235(3)	0.475(2)	0.037(1)
O(6)	−0.079(2)	0.376(1)	0.617 0(9)	C(19)	−0.282(2)	0.543(1)	−0.005(1)
O(7)	0.544(2)	0.310(1)	0.726(1)	C(20)	−0.211(2)	0.643(1)	0.027(1)
O(8)	0.696(2)	0.387 4(9)	0.470 2(9)	C(21)	−0.091(2)	0.687(1)	0.102(1)
O(9)	0.298(2)	0.506(1)	0.655 6(9)	C(22)	−0.048(2)	0.616(2)	0.149(1)
N(1)	0.159(1)	0.296 4(7)	0.362 5(7)	C(23)	−0.262(2)	0.702(1)	−0.025(1)
N(2)	−0.091(2)	0.440(1)	0.159(1)	C(24)	−0.404(2)	0.676(1)	−0.090(1)
C(1)	0.382(2)	−0.008(1)	0.383(1)	C(25)	−0.403(2)	0.757(2)	−0.124(1)
C(2)	0.158(2)	0.042(1)	0.272(1)	C(26)	−0.274(2)	0.826(1)	−0.083(1)
C(3)	0.476(2)	0.144 3(9)	0.313 1(9)	C(27)	−0.174(2)	0.801(1)	−0.017(1)
C(4)	−0.129(2)	0.110(1)	0.445(1)	C(28)	−0.405(3)	0.942(2)	0.136(2)
C(5)	0.076(2)	0.152(1)	0.617(1)	C(29)	−0.425(3)	0.863(2)	0.164(2)
C(6)	−0.022(2)	0.304(1)	0.575(1)	C(30)	−0.555(3)	0.798(2)	0.119(1)
C(7)	0.484(2)	0.303(1)	0.654(1)	C(31)	−0.646(3)	0.821(2)	0.056(2)
C(8)	0.582(2)	0.357(1)	0.501(1)	C(32)	−0.545(3)	0.922(2)	0.073(2)
C(9)	0.331(2)	0.428(1)	0.610(1)				

Table 8 Atomic coordinates for compound **3** with (e.s.d.s) in parentheses

Atom	x	y	z	Atom	x	y	z
Os(1)	0.324 93(5)	0.417 84(4)	0.691 54(8)	C(16)	0.138(1)	0.129 3(9)	0.811(2)
Os(2)	0.195 57(5)	0.462 02(4)	0.853 52(8)	C(17)	0.078(1)	0.201 4(8)	0.513(2)
Os(3)	0.134 22(5)	0.418 18(4)	0.517 94(8)	C(18)	0.157(1)	0.180 3(9)	0.484(2)
Fe	−0.146 8(2)	0.151 0(1)	0.727 6(3)	C(19)	0.142(1)	0.140(1)	0.337(2)
P(1)	0.102 8(3)	0.259 8(2)	0.698 9(5)	C(20)	0.052(1)	0.121(1)	0.220(2)
P(2)	−0.294 9(3)	0.070 0(3)	0.338 1(5)	C(21)	−0.028(1)	0.140 9(10)	0.249(2)
O(1)	0.355(1)	0.309 1(8)	0.453(2)	C(22)	−0.017(1)	0.180 9(9)	0.392(2)
O(2)	0.489(1)	0.387 3(9)	0.950(2)	C(23)	−0.015(1)	0.247 1(8)	0.748(2)
O(3)	0.461(1)	0.561 1(10)	0.592(2)	C(24)	−0.028(1)	0.235 5(9)	0.894(2)
O(4)	0.310(1)	0.443 4(9)	1.179(2)	C(25)	−0.124(1)	0.240 0(10)	0.902(2)
O(5)	0.251(1)	0.636 9(9)	0.971(2)	C(26)	−0.173(1)	0.254 6(10)	0.756(2)
O(6)	−0.015(1)	0.422 3(8)	0.919(2)	C(27)	−0.109(1)	0.259 3(9)	0.658(2)
O(7)	0.208(1)	0.560 1(9)	0.367(2)	C(28)	−0.139(1)	0.044(1)	0.762(2)
O(8)	−0.103(1)	0.372 5(8)	0.381(2)	C(29)	−0.223(1)	0.052(1)	0.801(2)
O(9)	0.135(1)	0.315 3(8)	0.239(2)	C(30)	−0.290(1)	0.063 3(10)	0.666(2)
C(1)	0.341(1)	0.350(1)	0.546(2)	C(31)	−0.244(1)	0.063 3(9)	0.543(2)
C(2)	0.427(2)	0.400(1)	0.855(2)	C(32)	−0.148(1)	0.050 4(9)	0.605(2)
C(3)	0.415(1)	0.508(1)	0.638(2)	C(33)	−0.367(1)	0.135 4(9)	0.351(2)
C(4)	0.262(1)	0.448(1)	1.054(2)	C(34)	−0.325(1)	0.210(1)	0.313(2)
C(5)	0.229(1)	0.571(1)	0.929(2)	C(35)	−0.366(2)	0.266(1)	0.336(2)
C(6)	0.065(1)	0.435(1)	0.898(2)	C(36)	−0.448(2)	0.251(1)	0.391(2)
C(7)	0.179(2)	0.509(1)	0.427(2)	C(37)	−0.497(2)	0.179(1)	0.418(2)
C(8)	−0.014(2)	0.389(1)	0.434(2)	C(38)	−0.457(1)	0.121(1)	0.398(2)
C(9)	0.133(1)	0.352(1)	0.348(2)	C(39)	−0.396(1)	−0.027(1)	0.265(2)
C(10)	0.173(1)	0.357 1(8)	0.707(2)	C(40)	−0.492(2)	−0.043(1)	0.166(2)
C(11)	0.170(1)	0.212 0(9)	0.836(2)	C(41)	−0.564(2)	−0.118(1)	0.094(3)
C(12)	0.257(1)	0.257(1)	0.964(2)	C(42)	−0.533(2)	−0.178(1)	0.129(3)
C(13)	0.307(2)	0.218(1)	1.067(2)	C(43)	−0.440(2)	−0.171(1)	0.225(3)
C(14)	0.276(1)	0.139(1)	1.041(2)	C(44)	−0.370(2)	−0.093(1)	0.298(2)
C(15)	0.193(1)	0.096(1)	0.918(2)				

temperature and evaporated to dryness. It was then redissolved in 5% aqueous NaOH (50 cm^3) and CH_2Cl_2 (200 cm^3). The organic phase was washed three times with H_2O (150 cm^3), dried over $MgSO_4$ and evaporated to dryness. The waxy residue is converted to a more stable microcrystalline solid by redissolution in diethyl ether and then evaporation to dryness. Purification of the crude mixture was accomplished by column chromatography on alumina. Elution with *n*-hexane–ether (80:20, v/v) first gave a yellow side-product and the pure product **I** was eluted as an orange band using acetone–CH_2Cl_2 (50:50, v/v) as eluent. Yield 0.63 g (49%) (Found: C, 74.55; H, 5.20; N, 4.05%; M^+, 339. Calc. for $C_{21}H_{17}FeN$: C, 74.35; H, 5.00; N, 4.15%; M^+, 339). ^1H NMR (CD_2Cl_2): δ 8.62 (2 H, m, J_{ab} 6.1, H_a), 7.63–7.48 (6 H, m, H_b, H_c and H_d), 4.72 (2 H, t, $J_{\alpha\beta}$ 2.0, H_α), 4.38 (2 H, t, $J_{\beta\alpha}$ 2.0 Hz, H_β), 4.06 (5 H, s, C_5H_5).

Preparation of p-*Bromo*-N-(4-*pyridylmethylene*)*aniline*.—A mixture of pyridine-4-carbaldehyde (2.77 cm^3, 0.03 mol) and 4-bromoaniline (5.00 g, 0.03 mol) in absolute ethanol (30 cm^3) as solvent was stirred under reflux for 2 h. The Schiff base that separated on cooling was filtered off and washed with cold ethanol. The crude product was purified by repeated recrystallisations from ethanol (yield 5.8 g, 77%). IR (Nujol): 1619 cm^{-1} ($\nu_{C=N}$) (Found: C, 55.60; H, 3.50; N, 10.70%; M^+, 260. Calc. for $C_{12}H_9BrN_2$: C, 55.40; H, 3.45; N, 10.75%; M^+, 260). ^{1}H NMR ($CDCl_3$): δ 8.76 (2 H, m, J_{ab} 5.9, H_a), 8.43 (1 H, s, CH=N), 7.74 (2 H, m, J_{ba} 5.9, H_b), 7.53 (2 H, m, J_{cd} 9.0, H_c), 7.12 (2 H, m, J_{dc} 9.0 Hz, H_d).

Preparation of $[Fe(\eta^5\text{-}C_5H_5)(\eta^5\text{-}C_5H_4C_6H_4N{=}CHC_5H_4N)]$ **II**.—This compound was synthesised using the conditions described for **I** but *p*-bromo-*N*-(4-pyridylmethylene)aniline (0.65 g, 2.50 mmol) was used instead of 4-(*p*-bromophenyl)-pyridine. Yield: 0.64 g (46%). IR (Nujol): 1619 cm^{-1} ($\nu_{C=N}$) (Found: C, 72.30; H, 4.75; N, 7.45%; M^+, 366. Calc. for $C_{22}H_{18}FeN_2$: C, 72.15; H, 4.90; N, 7.65%; M^+, 366). ^{1}H NMR (CD_2Cl_2): δ 8.73 (2 H, m, J_{ab} 6.1, H_a), 8.56 (1 H, s, CH=N), 7.77 (2 H, m, J_{ba} 6.1, H_b), 7.55 (2 H, m, J_{cd} 8.6, H_c), 7.24 (2 H, m, J_{dc} 8.6, H_d), 4.69 (2 H, t, $J_{\alpha\beta}$ 2.0, H_α), 4.36 (2 H, t, $J_{\beta\alpha}$ 2.0 Hz, H_β), 4.05 (5 H, s, C_5H_5).

Preparation of $[Os_3(\mu\text{-}H)_2(CO)_9\{\mu_3\text{-}CNC_5H_4C_6H_4(\eta^5\text{-}C_5H_4)Fe(\eta^5\text{-}C_5H_5)\}]$ **1**.—The compound $[Os_3(\mu\text{-}H)_3(CO)_9(\mu_3\text{-}CCl)]$ (87.3 mg, 0.10 mmol) and the ferrocenyl ligand **I** (0.34 g, 1.00 mmol) in CH_2Cl_2 (15 cm^3) were stirred at room temperature. Dropwise addition of a dbu–CH_2Cl_2 solution (0.10 mmol) gave a deep red solution. The mixture was stirred for 30 min and subsequently evaporated to dryness under vacuum. The residue was purified by TLC using *n*-hexane–CH_2Cl_2 (75:25, v/v) as eluent. Complex **1** was isolated as a red major product (R_f = 0.40) in 42% yield (49 mg). IR (CH_2Cl_2): ν_{CO}/cm^{-1} 2088m, 2053vs, 2022vs, 1981s, 1948m, 1932m [Found: C, 31.95; H, 1.70; N, 1.25%; M^+, 1177. Calc. for $C_{31}H_{19}FeNO_9Os_3$: C, 31.60; H, 1.60; N, 1.20%; M^+, 1177 (simulated *m*/*z*)]. ^{1}H NMR (CD_2Cl_2): δ 9.57 (2 H, m, J_{ab} 7.1, H_a), 7.76 (2 H, m, J_{cd} 8.5, H_c), 7.70 (2 H, m, J_{ba} 7.1, H_b), 7.65 (2 H, m, J_{dc} 8.5, H_d), 4.78 (2 H, t, $J_{\alpha\beta}$ 1.9, H_α), 4.45 (2 H, t, $J_{\beta\alpha}$ 1.9 Hz, H_β), 4.07 (5 H, s, C_5H_5), −18.95 (2 H, s, OsH).

Preparation of $[Os_3(\mu\text{-}H)_2(CO)_9\{\mu_3\text{-}CNC_5H_4CH{=}NC_6H_4(\eta^5\text{-}C_5H_4)Fe(\eta^5\text{-}C_5H_5)\}]$ **2**.—To a solution of $[Os_3(\mu\text{-}H)_3(CO)_9(\mu_3\text{-}CCl)]$ (87.3 mg, 0.10 mmol) and the ferrocenyl ligand **II** (0.37 g, 1.0 mmol) in CH_2Cl_2 (15 cm^3) was added dbu (1 equivalent) and the mixture stirred for 30 min. The mixture was evaporated to dryness and chromatographed by TLC using *n*-hexane–CH_2Cl_2 (70:30, v/v) as eluent. A major product was isolated from the blue band (R_f = 0.60) and was characterised as **2** in 40% yield (48 mg). IR (CH_2Cl_2): ν_{CO}/cm^{-1} 2089m, 2055vs, 2024vs, 1983s, 1951m, 1935m [Found: C, 31.65; H, 1.55; N, 2.30%; M^+, 1204. Calc. for $C_{32}H_{20}FeN_2O_9Os_3$: C, 31.90; H, 1.65; N, 2.35%; M^+, 1204 (simulated *m*/*z*)]. ^{1}H NMR (CD_2Cl_2): δ 9.71 (2 H, m, J_{ab} 6.8, H_a), 8.65 (1 H, s, CH=N), 7.89 (2 H, m, J_{ba} 6.8, H_b), 7.57 (2 H, m, J_{cd} 8.5, H_c), 7.37 (2 H, d, J_{dc} 8.5, H_d), 4.72 (2 H, t, $J_{\alpha\beta}$ 1.9, H_α), 4.40 (2 H, t, $J_{\beta\alpha}$ 1.9 Hz, H_β), 4.06 (5 H, s, C_5H_5), −18.83 (2 H, s, OsH).

Preparation of $[Os_3(\mu\text{-}H)_2(CO)_9\{\mu_3\text{-}CPPh_2(\eta^5\text{-}C_5H_4)Fe(\eta^5\text{-}C_5H_4PPh_2)\}]$ **3**.—The complex $[Os_3(\mu\text{-}H)_3(CO)_9(\mu_3\text{-}CCl)]$ (87.3 mg, 0.10 mmol) and an excess of $[Fe(\eta^5\text{-}C_5H_4PPh_2)_2]$ (0.55 g, 1.00 mmol) were dissolved in CH_2Cl_2 (15 cm^3) and a dbu–CH_2Cl_2 solution (0.10 mmol) was added dropwise. The yellow-orange reaction mixture was stirred at room temperature for 30 min. Solvent was removed under vacuum and the residue was chromatographed by TLC using *n*-hexane–acetone (90:10, v/v) to afford complex **3** as an orange-yellow solid (R_f = 0.60) in 32% yield (45 mg). IR (CH_2Cl_2): ν_{CO}/cm^{-1} 2093s, 2055vs, 2024vs, 2014 (sh), 2001 (sh), 1979s, 1951m, 1936m [Found: C, 37.80; H, 2.20%; M^+, 1392. Calc. for $C_{44}H_{30}FeO_9Os_3P_2$: C, 37.95; H, 2.15%; M^+, 1392 (simulated *m*/*z*)]. ^{1}H NMR (CD_2Cl_2): δ 7.49–8.11 (10 H, m, phenyl), 7.32 (10 H, m, phenyl), 4.38 (2 H, m, C_5H_4), 4.31 (2 H, m, C_5H_4), 4.07 (2 H, m, C_5H_4), 3.94 (2 H, m, C_5H_4), −19.88 (2 H, d, $^3J_{HP}$ 2.8 Hz, OsH). ^{31}P NMR (CD_2Cl_2): δ 41.82 (s), −17.04 (s).

X-Ray Data Collection, Solution and Refinement.—Single crystals of **1** suitable for X-ray analysis were obtained by slow evaporation of a *n*-heptane–$CHCl_3$ solution at room temperature for a period of 3 d. Single crystals of **2** and **3** suitable for X-ray experiments were grown by slow evaporation of their respective solutions in *n*-hexane–CH_2Cl_2 at ambient temperatures for 2 d. The unit-cell parameters of the compounds were obtained from setting angles of 25 accurately centred reflections. The choice of space group was based on systematically absent reflections and confirmed by the successful solution and refinement of the structure. All pertinent crystallographic data are summarised in Table 5. Data were collected at room temperature on either an Enraf-Nonius CAD4-diffractometer (for **2**) or a Rigaku AFC7R diffractometer (for **1** and **3**) with graphite-monochromatised Mo-Kα radiation (λ = 0.710 73 Å) using the ω–2θ scan technique. The stability of the crystals was monitored at regular intervals using three standard reflections and no significant variation was observed. Intensity data were corrected for Lorentz and polarisation effects and semi-empirical absorption corrections (ψ-scan method) were also applied.[36] Scattering factors were taken from ref. 37(*a*) and anomalous dispersion effects[37b] were included in F_c.

The structures were solved by a combination of direct methods (SIR 88[38] for **1** and **3**, MULTAN 82[39] for **2**) and Fourier difference techniques and refined on *F* by full-matrix least-squares analysis. The hydrogen atoms of the organic moieties were generated in their ideal positions (C–H 0.95 Å), while all metal hydrides were estimated by potential-energy calculations.[27] Calculations were performed either on a MicroVax II (**2**) or a Silicon-Graphics (**1** and **3**) computer using the Program packages SDP (from Enraf-Nonius)[40] or TEXSAN (from MSC).[41] Positional parameters for the non-hydrogen atoms are given in Tables 6–8.

Additional material available from the Cambridge Crystallographic Data Centre comprises H-atom coordinates, thermal parameters and remaining bond lengths and angles.

Acknowledgements

We gratefully acknowledge financial support from the Hong Kong Research Grants Council and the University of Hong Kong. W.-Y. W. thanks the Croucher Foundation for financial support.

References

1 E. C. Constable, R. Martinez-Manez, A. M. W. Cargill-Thompson and J. V. Walker, *J. Chem. Soc., Dalton Trans.*, 1994, 1585.
2 D. Astruc, *New J. Chem.*, 1992, **16**, 305.
3 J.-P. Collin, S. Guillerez, J.-P. Sauvage, F. Barigelletti, L. D. Cola, L. Flamigui and V. Balzani, *Inorg. Chem.*, 1991, **30**, 4230.
4 J.-P. Collin, S. Guillerez and J.-P. Sauvage, *J. Chem. Soc., Chem. Commun.*, 1989, 776.
5 M. L. H. Green, S. R. Marder, M. E. Thompson, J. A. Bandy, D. Bloor, P. V. Kolinsky and R. J. Jones, *Nature* (*London*), 1987, **330**, 360.
6 A. Houlton, S. K. Ibrahim, J. R. Dilworth and J. Silver, *J. Chem. Soc., Dalton Trans.*, 1990, 2421.
7 P. D. Beer, J. E. Nation, S. W. L. McWhinnie, M. E. Harman, M. B. Hursthouse, M. I. Ogden and A. H. White, *J. Chem. Soc., Dalton Trans.*, 1991, 2485.
8 R. Wagner, P. A. Brown, T. E. Johnson and J. S. Lindsey, *J. Chem. Soc., Chem. Commun.*, 1991, 1463.
9 J. S. Miller, A. J. Epstein and W. M. Reiff, *Chem. Rev.*, 1988, **88**, 201.
10 C. Kollmar, M. Couty and O. Kahn, *J. Am. Chem. Soc.*, 1991, **113**, 7994.
11 B. Delavaux-Nicot, R. Mathieu, D. de Montauzon, G. Lavigne and J.-P. Majoral, *Inorg. Chem.*, 1994, **33**, 434.
12 See, for example, S. R. Marder, *Inorganic Materials*, eds. D. W. Bruce and D.O'Hare, Wiley, Chichester, 1992, p. 136; M. C. B. Colbert, A. J. Edwards, J. Lewis, N. J. Long, N. A. Page, D. G. Parker and P. R. Raithby, *J. Chem. Soc., Dalton Trans.*, 1994, 2589; K. L. Kott, D. A. Higgins, R. J. McMahon and R. L. Corn, *J. Am. Chem. Soc.*, 1993, **115**, 5342; A. Benito, J. Cano, R. Martinez-

Manez, J. Paya, J. Soto, M. Julve, F. Lloret, M. D. Marcos and E. Sinn, *J. Chem. Soc., Dalton Trans.*, 1993, 1999; B. J. Coe, C. J. Jones, J. A. McCleverty, D. Bloor and G. Cross, *J. Organomet. Chem.*, 1994, **464**, 225; S. Ghosal, M. Samoc, P. N. Prasad and J. J. Tufariello, *J. Phys. Chem.*, 1990, **94**, 2847; Z. Yuan, N. J. Taylor, Y. Sun, T. B. Marder, I. D. Williams and L.-T. Cheng, *J. Organomet. Chem.*, 1993, **449**, 27; Z. Yuan, G. Stringer, T. R. Jobe, D. Kreller, K. Scott, L. Koch, N. J. Taylor and T. B. Marder, *J. Organomet. Chem.*, 1993, **452**, 115.

13 J. C. Medina, I. Gay, Z. Chen, L. Echegoyen and G. W. Gokel, *J. Am. Chem. Soc.*, 1991, **113**, 365.

14 A. Werner and W. Friedrichsen, *J. Chem. Soc., Chem. Commun.*, 1994, 365.

15 R. Deschenaux, I. Kosztics, U. Scholten, D. Guillon and M. Ibn-Elhaj, *J. Mater. Chem.*, 1994, **4**(8), 1351.

16 M. V. Russo, A. Furlani, S. Licoccia, R. Paolesse, A. C. Villa and C. Guastini, *J. Organomet. Chem.*, 1994, **469**, 245.

17 M. Sato, H. Shintate, K. Kawata, M. Sekino, M. Katada and S. Kawata, *Organometallics*, 1994, **13**, 1956.

18 S. Chan, W. Y. Wong and W. T. Wong, *J. Organomet. Chem.*, 1994, **474**, C30.

19 B. F. G. Johnson, F. J. Lahoz, J. Lewis, N. D. Prior, P. R. Raithby and W. T. Wong, *J. Chem. Soc., Dalton Trans.*, 1992, 1701.

20 J.-C. Chambron, C. Coudret and J.-P. Sauvage, *New J. Chem.*, 1992, **16**, 361.

21 J.-M. Lehn, *Angew. Chem., Int. Ed. Engl.*, 1990, **29**, 1304.

22 C. Amatore, A. Jutand and S. Negri, *J. Organomet. Chem.*, 1990, **390**, 389.

23 V. Balzani and F. Scandola, *Supramolecular Photochemistry*, Ellis Horwood, Chichester, 1991, chs. 3 and 5.

24 W. T. Wong and W. Y. Wong, *Acta Crystallogr., Sect. C*, in the press.

25 J. R. Shapley, M. E. Cree-Uchiyama, G. M. St. George, M. R. Churchill and C. Bueno, *J. Am. Chem. Soc.*, 1983, **105**, 140.

26 I. R. Butler and W. R. Cullen, *Organometallics*, 1986, **5**, 2537.

27 A. G. Orpen, *J. Chem. Soc., Dalton Trans.*, 1980, 2509.

28 M. R. Churchill and B. G. DeBoer, *Inorg. Chem.*, 1977, **16**, 878.

29 C. Lopez, J. Sales, X. Solans and R. Zquiak, *J. Chem. Soc., Dalton Trans.*, 1992, 2321.

30 A. L. Abuhijleh and C. Woods, *J. Chem. Soc., Dalton Trans.*, 1992, 1249.

31 C. E. Housecoft, personal communication.

32 E. Buncel and S. Rajagopal, *Acc. Chem. Res.*, 1990, **23**, 226.

33 R. W. Fish and M. Rosenblum, *J. Org. Chem.*, 1965, **30**, 1253.

34 P. Boy, C. Combellas, A. Thiebault, C. Amatore and A. Jutand, *Tetrahedron Lett.*, 1992, **33**, 491.

35 J. B. Keister and T. L. Horling, *Inorg. Chem.*, 1980, **19**, 2304.

36 A. C. T. North, D. C. Phillips and F. S. Mathews, *Acta Crystallogr., Sect. A*, 1968, **24**, 351.

37 D. T. Cromer and J. T. Waber, *International Tables for X-Ray Crystallography*, Kynoch Press, Birmingham, 1974, vol. 4, (*a*) Table 2.2B; (*b*) Table 2.3.1.

38 M. C. Burla, M. Camalli, G. Cascarano, C. Giacovazzo, G. Polidori, R. Spagna and D. Viterbo, *J. Appl. Crystallogr.*, 1989, **22**, 389.

39 P. Mains, S. J. Fiske, S. E. Hull, L. Lessinger, G. Germain, J. P. Declercq and M. M. Woolfson, MULTAN 82, A System of Computer Programs, for the Automatic Solution of Crystal Structures, Universities of York and Louvain, 1991.

40 SDP Structure Determination Package, Enraf-Nonius, Delft, 1985.

41 TEXSAN: Crystal Structure Analysis Package, Molecular Structure Corporation, Houston, TX, 1985 and 1992.

Received 9*th November* 1994; *Paper* 4/06842D